

ARTICLE OPEN



Challenges with interpreting the impact of Atlantic Multidecadal Variability using SST-restoring experiments

Christopher H. O'Reilly¹✉, Matthew Patterson², Jon Robson³, Paul Arthur Monerie³, Daniel Hodson³ and Yohan Ruprich-Robert⁴

Climate model simulations that restore SSTs in the North Atlantic have been used to explore the climate impacts of Atlantic Multidecadal Variability (AMV). However, despite simulations and observations exhibiting similar North Atlantic SST anomalies, experiments with active SST-restoring in the Tropical North Atlantic exhibit strong positive surface heat-fluxes out of the ocean with warm SST anomalies, which is not replicated in other simulations or observations. The upward surface heat-fluxes that are systematically driven by the active SST-restoring in the Tropical North Atlantic are found to be crucial for generating a strong local precipitation response and the associated remote impact on the Pacific Walker circulation; these are both absent in other simulations. The results of this study strongly suggest that experiments employing SST-restoring (or prescribed SSTs) in the Tropical North Atlantic exaggerate the influence of the Atlantic on patterns of global climate anomalies and its role in recent multidecadal SST trends.

npj Climate and Atmospheric Science (2023)6:14; <https://doi.org/10.1038/s41612-023-00335-0>

INTRODUCTION

Over the past 150 years or so the observed variability of sea surface temperatures (SSTs) over the North Atlantic has exhibited substantial variability on multidecadal timescales, which is often referred to as the Atlantic Multidecadal Oscillation or Atlantic Multidecadal Variability (AMV)^{1–4}. The AMV has been linked to significant multidecadal variability in surrounding continental climate regions, including over North America^{5–11}, Europe^{12–16} and the Sahel^{17–20}. The AMV has also been linked to remote influences over the Pacific and East Asia^{21–26}. Understanding the influence of the North Atlantic on regional climate is therefore important for understanding and predicting climate variability.

Due to the relatively short observational record, many of the studies aiming to understand the impact of the AMV on regional climate variability have consisted of modelling studies to isolate and characterise the influence of the AMV. One common method is to prescribe SST boundary conditions in an atmospheric general circulation model and analyse the resulting climate influence of the AMV^{12,27–29}. One drawback of using a prescribed SST boundary condition is that coupled ocean-atmosphere interactions are poorly represented and at any one location the ocean can act as an unrealistic source/sink of heat to the overlying atmosphere³⁰.

A relatively recent development that has been used to avoid the issues around prescribed SSTs has been the use of coupled models in which SSTs are nudged towards some target value. An example of these are *transient pacemaker experiments*, in which the temperatures in the upper-ocean mixed-layer are forced towards a prescribed and evolving temperature anomaly in a particular region³¹. A more idealised approach, which has been used to assess the impact of the AMV are *SST-restoring experiments* (referred to “idealised pacemaker experiments” in some studies) in which SSTs are restored towards a time-invariant SST anomaly pattern across the North Atlantic^{23,32,33}. The aim of these simulations is to determine the influence of the SST anomalies

on the broader climate system without breaking the coupled interactions between the atmosphere and ocean and should therefore be superior to prescribing SSTs in an atmosphere-only simulation. Recent studies using SST-restoring simulations have demonstrated an important influence of the North Atlantic on the large-scale circulation over the North Atlantic sector but also remote influences over the Pacific and Asia. Perhaps the most striking impact of the AMV in these simulations is the influence on the Tropical Pacific and the further associated impacts^{23,33–39}.

SST-restoring experiments have been widely used to directly attribute how AMV can affect global climate, however, it is not clear that these SST-restoring experiments appropriately represent the ocean-atmosphere interaction over the North Atlantic on decadal timescales. In this study, we specifically analyse the surface heat-fluxes and associated atmospheric response in SST-restoring simulations and demonstrate that, in some cases, these differ substantially from the behaviour seen in free-running coupled models and long observational/reanalysis datasets. These results have implications for interpreting the role of AMV on regional climate anomalies and global SST trend patterns in recent decades.

RESULTS

SST and heat-flux relationships in SST-restoring experiments and free-running coupled models

In this section we analyse the SSTs and surface heat-fluxes associated with AMV in SST-restoring experiments, in which the SSTs are relaxed to a target AMV SST pattern, in free-running coupled model simulations (i.e. CMIP6 piControl and historical) and in observational datasets (see Methods). We begin our analysis by examining the differences (i.e. AMV positive minus AMV negative) between the SSTs in SST-restoring experiments (Fig. 1 & Table 1). The IPSL and UM SST-restoring experiments generally show similar SST differences in all the experiments,

¹Department of Meteorology, University of Reading, Reading, UK. ²Department of Physics, University of Oxford, Oxford, UK. ³National Centre for Atmospheric Science, University of Reading, Reading, UK. ⁴Barcelona Supercomputing Center, Barcelona, Spain. ✉email: c.h.oreilly@reading.ac.uk

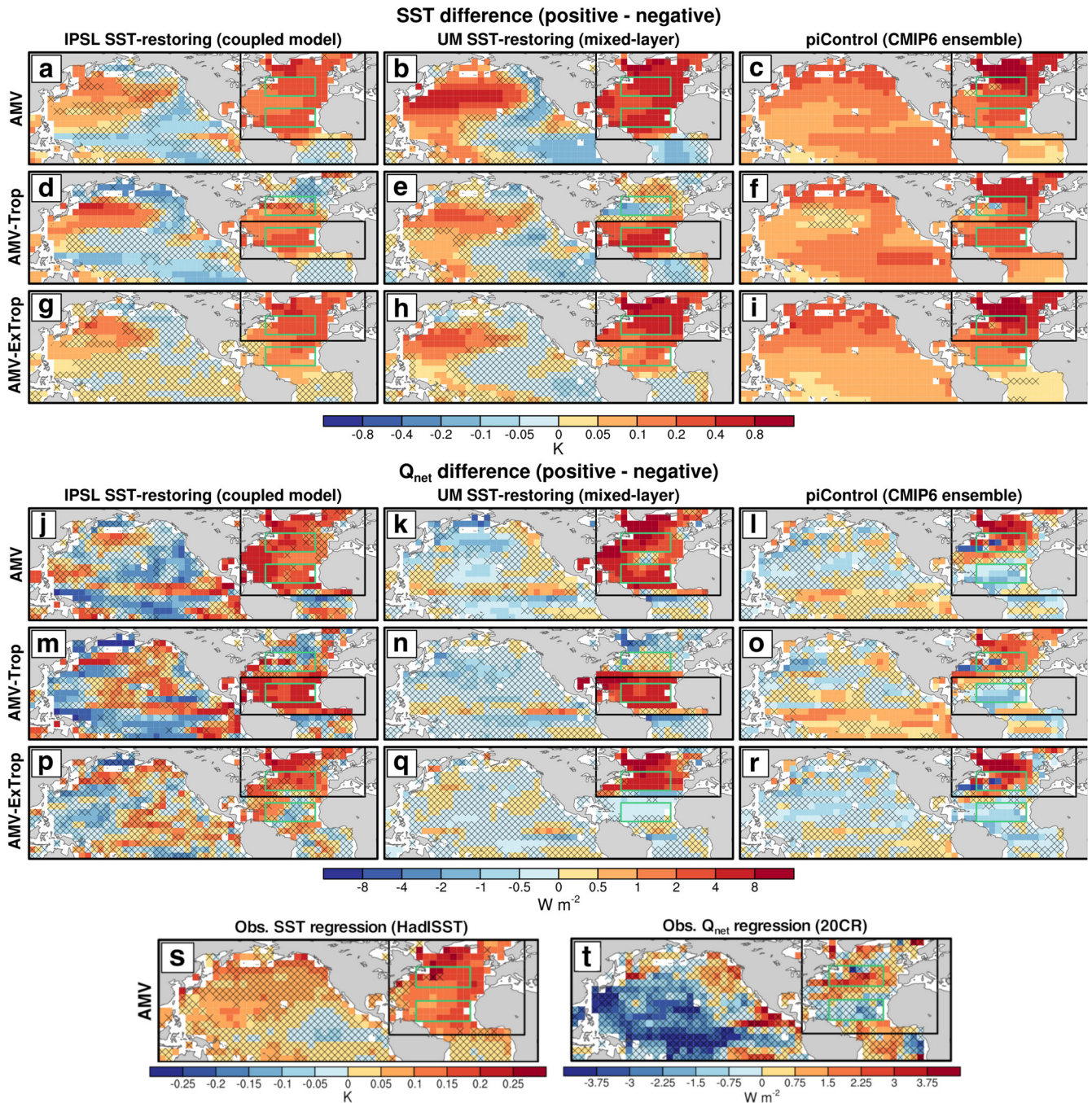


Fig. 1 The dependence of SST and surface heat-flux on AMV phase. **a–i** SST difference between SST+ and SST- 10-year periods for the AMV, AMV-Trop and AMV-ExTrop regions (indicated by the black boxes). These are shown for the SST-restoring experiments for the IPSL and UM models; for the free-running coupled PiControl simulations the SST+ and SST- decades are decades in which the SST in the region is above/below one standard deviation from the mean. **j–r** Surface heat-flux, Q_{net} (defined as positive upwards), difference between SST+ and SST- 10-year periods for the AMV, AMV-Trop and AMV-ExTrop regions. Hatching indicates where the differences are not significant at the 95% level, based on a Monte Carlo resampling performed 10000 times (see Methods). **s** Decadal SST anomalies (HadISST, 1870–2014) and **t** Q_{net} anomalies (20CR, 1870–2014) regressed onto a normalised decadal SST index averaged over the AMV region. Hatching in **(s, t)** indicates where the regression coefficients are not significant at the 95% level, based on a Monte Carlo phase randomisation test (see Methods). The green boxes indicate the midlatitude and subtropical North Atlantic regions used in Fig. 2.

albeit largely by design over the North Atlantic. In the AMV and AMV-ExTrop experiments, the SST differences are significantly positive across the entire North Atlantic (Fig. 1a, b, g, h), whereas in the AMV-Trop experiments the positive differences are mostly limited to the subtropical region in which the relaxation is applied (Fig. 1d, e). The difference between the analogous positive and negative periods in the free-running piControl simulations are

similar across all three index regions over the North Atlantic (Fig. 1c, f, h) and are most similar to the AMV and AMV-ExTrop SST-restoring simulations. The differences in the free-running piControl simulations are also similar to the observed SST anomaly pattern associated with the AMV, which are shown in Fig. 1s (and is similar for all regions and is also similar in the CMIP6 Historical simulations; Supplementary Fig. 2).

Table 1. Summary of the simulations analysed in this study.

Simulation name	External forcing	SSTs	Length/period	Ens. size	Model
IPSL SST-restoring	Preindustrial control	Dynamical ocean model with SST-restoring towards fixed anomalies in specified regions.	10 years	25	IPSL-CM6
UM SST-restoring	Preindustrial control	Mixed-layer ocean model with SST-restoring towards fixed anomalies in specified regions.	10 years	10	MetUM-GOML
CMIP6 Historical	Historical forcing	Free-running coupled model simulations.	1870–2014	318	Various models (CMIP6).
CMIP6 piControl	Preindustrial control	Free-running coupled model simulations.	250–1200 years	16	Various models (CMIP6).
Transient pacemaker	Historical forcing	Dynamical ocean model with SST-restoring towards varying (i.e. transient) observed anomalies in specified regions.	1920–2014	10	IPSL-CM6
AMIP-hist	Historical forcing	Atmospheric model simulations with prescribed observed SSTs.	1870–2014	49	Various models (CMIP6).

To examine how these SST anomalies interact with the atmosphere we now examine the differences in surface heat flux, Q . This is defined here as the net surface heat flux due to long and shortwave radiative fluxes and latent and sensible turbulent heat fluxes with positive values being out of the ocean. The surface heat flux differences between the positive and negative SST-restoring experiments (Fig. 1j–r) are generally positive in the regions in which the temperature anomalies are being forced in the SST-restoring simulations: the surface heat flux differences are positive over the whole North Atlantic in the AMV runs, positive over the tropical North Atlantic in the AMV-Trop runs, and positive over the extratropical North Atlantic in the AMV-ExTrop runs. One notable feature is the very different surface heat fluxes in the subtropical North Atlantic region in the AMV and AMV-ExTrop simulations, positive in the AMV experiments and small and generally negative in the AMV-ExTrop experiments, this is despite exhibiting similar SST differences in this region. In contrast to the SST-restoring experiments, the difference between the positive and negative periods in the free-running piControl simulations are similar across all three index regions and exhibit a pattern that most resembles the AMV-ExTrop SST-restoring experiments, with positive values in the extra-tropics and negative values in the subtropics.

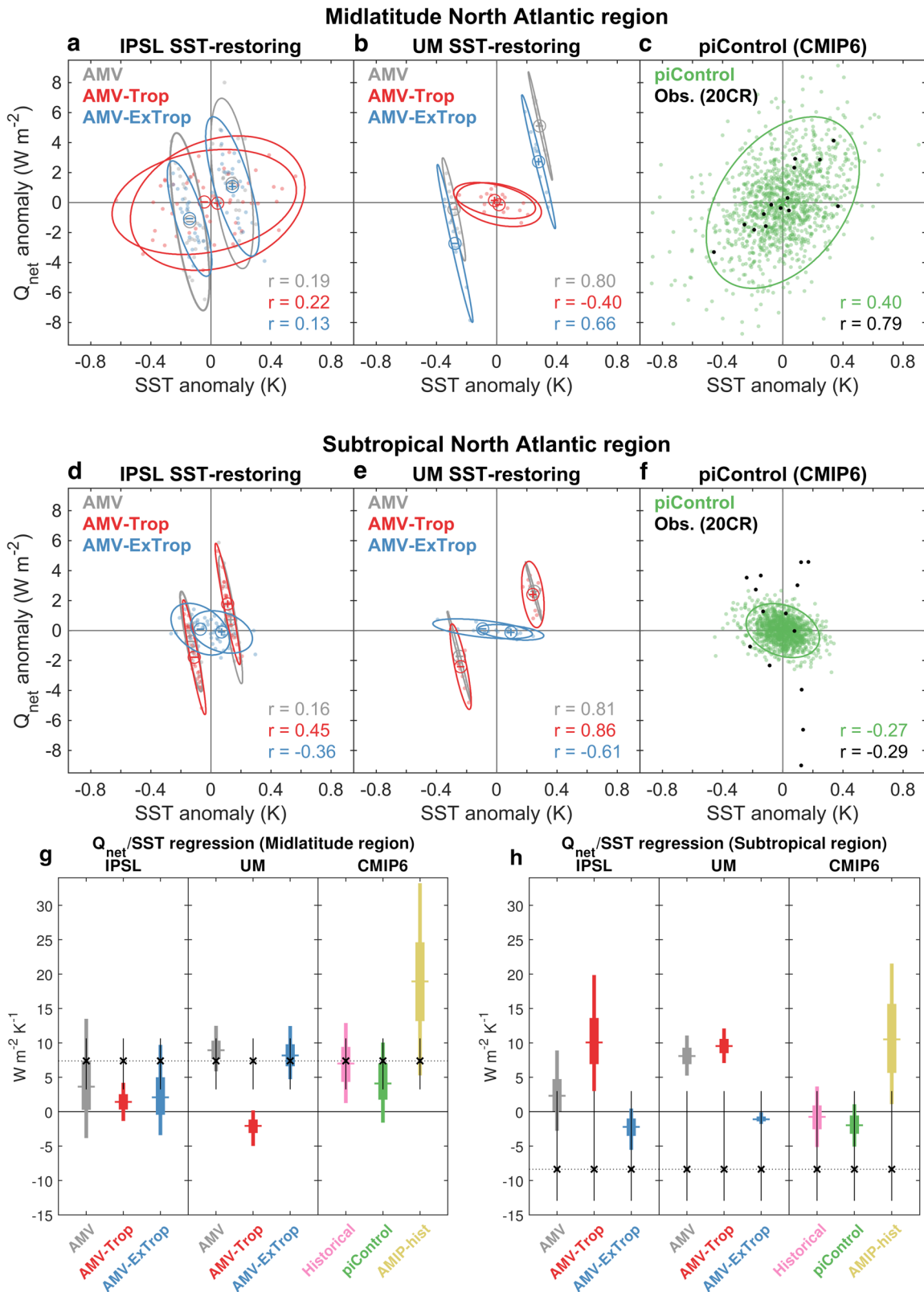
We can investigate the relationship between decadal SST and surface heat-flux anomalies in more detail for midlatitude and subtropical North Atlantic regions by examining the scatter plots shown in Fig. 2 (and Supplementary Fig. 3 for scatter plots from the CMIP6 Historical simulations). The equivalent decadal anomalies for the observational datasets are shown by the black dots in Fig. 2c, f; we show heat-flux data from 20CR but analysis of an alternative, albeit shorter, observational dataset (OAflux) demonstrates broadly similar behaviour (Supplementary Fig. 6). Here we examine the surface heat-flux anomalies but these are dominated by turbulent heat-fluxes and similar results are found if only turbulent heat-flux components are analysed (see Supplementary Figs. 4, 5, 8 & 9). To compare across the different simulations more directly, we computed linear regression coefficients between the surface heat-flux anomalies (Q_{net}) and SST in the midlatitude and subtropical North Atlantic regions (shown in Fig. 2g, h). The regression coefficients were calculated in 140-year periods by randomly sampling decades from the SST-restoring experiments and across all different ensemble periods/members in the free-running piControl, Historical and AMIP-hist simulations.

In the midlatitude North Atlantic there is a positive relationship between the decadal SST and surface heat flux anomalies in the SST-restoring experiments with active restoring (i.e. AMV & AMV-

ExTrop), in all the free-running simulations and in the observations, indicating that the surface heat fluxes are acting to damp the SST anomalies. The only exception is the AMV-Trop experiment in the UM slab-ocean model, which has no active SST-restoring in this region so SSTs are passively forced by surface heat fluxes and the relationship is negative. The regression coefficients are all broadly the free-running models and AMV/AMV-ExTrop SST-restoring experiments are broadly consistent with the observations; a notable exception is the AMIP-hist simulation, which has an extremely strong positive relationship, consistent with the unrealistic SST damping expected from prescribed SSTs (see also the scatter plots in Supplementary Fig. 7). As such, despite there being a fairly wide range of possible behaviour, we can conclude that the systematic relationship between the decadal SST and surface heat flux anomalies in the AMV and AMV-ExTrop experiments are similar to the behaviour seen in observations and in free-running coupled models.

In the subtropical North Atlantic, however, there are major discrepancies between the SST-restoring experiments with active restoring (i.e. AMV & AMV-Trop) and the observations and free-running coupled models (Fig. 2d, e, f & Supplementary Fig. 3). The AMV and AMV-Trop experiments both exhibit systematically positive relationships between the decadal SST and surface heat flux anomalies in the subtropical North Atlantic, in contrast to the observations and free-running coupled model simulations, which overall exhibit weakly negative relationships. This is particularly clear in the regression plots (Fig. 2h), where it is only the AMV, AMV-Trop and AMIP-hist experiments that exhibit a positive heat-flux associated with positive SST anomalies in the subtropical North Atlantic region, whereas the other simulations - including the AMV-ExTrop experiments - exhibit a zero or weakly negative relationship, which is more consistent with the relationship estimated in the observational datasets.

It is also of interest to examine the seasonal dependence of the SST/surface heat-flux relationships (shown in Supplementary Figs. 11 & 12). In the midlatitude region there is a positive relationship throughout most of the year in the AMV, AMV-ExTrop and free-running piControl and Historical simulations. This is not well constrained in the observational datasets but is reasonably consistent. In the subtropical region, the AMV and AMV-Trop SST-restoring experiments show positive SST/surface heat-flux relationships throughout the year; this is inconsistent with the AMV-ExTrop SST-restoring simulations and free-running piControl and Historical simulations, which show a positive relationship in the summer period and a negative relationship in the winter period. The seasonally varying SST/surface heat-flux relationship in the subtropical region is consistent with the observational



estimates and is reminiscent of the response of the Tropical North Atlantic to wintertime El Niño event anomalies on seasonal timescales: SST anomalies are forced from the atmosphere in winter by negative surface heat-flux anomalies; these SST anomalies are then damped to the atmosphere through positive

surface heat-flux anomalies in the following summer⁴⁰. The seasonal dependence of the SST/surface heat-flux relationship show that the AMV and AMV-Trop SST-restoring experiments are more consistent with the other experiments and observational data in the boreal summer season, when the positive SST

Fig. 2 Relationships between SST and surface heat-flux in the midlatitude and subtropical North Atlantic. Scatter plots of decadal surface heat-flux (Q_{net}) anomalies (defined positive upwards) versus decadal SST anomalies over the midlatitude North Atlantic region (shown by green boxes in Fig. 1) for (a) the idealised IPSL pacemaker experiments, (b) the idealised UM pacemaker experiments, (c) *Historical* simulations, and (d) *piControl* simulations. Each dot shows a value averaged over a different 10-year period and simulation and the ellipses show the two-dimensional Gaussian probability density function calculated across all the dots shown. The black dots show the decadal anomalies from the observational datasets (i.e. HadISST and 20CR). (e, f) As in (a–c) but for anomalies over the subtropical North Atlantic region (shown by green boxes in Fig. 1). Also shown is the regression of decadal surface heat-flux anomalies onto decadal SST anomalies for (g) the midlatitude North Atlantic region and (h) the subtropical North Atlantic region. The regressions were calculated for all unique 140-year periods in the historical and *piControl* simulations and the box, centre-lines and whiskers show the 5th–25th–50th–75th–95th percentiles of these distributions. For the SST-restoring experiments 10000 random 140-year periods (i.e. 14 decades) were sampled and constructed from the ensemble members to calculate the regression; the box and whiskers show the distribution across these random samples for each experiment. The crosses and dotted lines show the equivalent regression coefficient calculated from the observational datasets. The vertical black lines are an estimate of the 5–95% confidence limits of the regression coefficient calculated from the observations, calculated using a block bootstrap resampling with replacement using a block length of 20-years (repeated 10,000 times).

anomalies drive upward surface heat-fluxes. The SST-restoring in the tropical North Atlantic may also be more realistic on interannual timescales, as SSTs in this region have been cited as an important precursor of ENSO events⁴¹. This indicates that the behaviour seen in the AMV & AMV-Trop SST-restoring experiments is likely more realistic in the boreal summer season than in the boreal winter season.

In this section we have identified some important characteristics of the SST-restoring experiments. The AMV-ExTrop experiment, with SST-restoring in the extratropical North Atlantic exhibits characteristics of ocean-atmosphere coupling on decadal timescales over the North Atlantic that are consistent with free-running coupled models and observations; more specifically, the decadal surface heat flux anomalies in the midlatitudes exhibit the same sign as the SST anomalies, whereas in the subtropics the heat-flux and SST anomalies have a weakly negative correlation (i.e. Fig. 2). However, in the experiments with active SST-restoring in the tropics, AMV and AMV-Trop experiments, decadal surface heat flux anomalies in the subtropical North Atlantic region exhibit the same sign as the SST anomalies and are therefore inconsistent with free-running coupled models and observations.

Links between the AMV and decadal precipitation anomalies

Several studies exploring the remote influence of the AMV on the climate system have emphasised the influence of the SST anomalies on anomalous precipitation, ascent and associated divergence at upper levels^{33,35}. The differences in precipitation rate between positive and negative SST periods in the SST-restoring experiments and analogous period are shown in Fig. 3a–i. The warmer SSTs are associated with more precipitation across most of the extra-tropics and the tropics in the North Atlantic. Particularly notable is the intensification of the Inter-tropical Convergence Zone (ITCZ) to the north of the equator in the Atlantic. Whilst the intensification of the precipitation in the Tropical North Atlantic region (shown by magenta box in Fig. 3) is present in all experiments, it is much stronger in the AMV and AMV-Trop experiments, in which there is active SST-restoring in the tropics. Comparison of the precipitation strength in the Tropical North Atlantic region in the SST-restoring and free-running ensembles, plotted in Fig. 3j, indicates that the experiments with active SST-restoring (i.e. AMV and AMV-Trop) can support substantially higher precipitation anomalies than in simulations without active SST-restoring.

To examine the relationship between the SSTs and the precipitation in the Tropical North Atlantic across the different simulations we computed linear regression coefficients between the decadal anomalies (shown in Fig. 3k). For the SST-restoring experiments, the precipitation response substantially higher in the experiments with active SST-restoring (i.e. AMV and AMV-Trop) - around double the magnitude of the simulations without active SST-restoring (i.e. AMV-ExTrop) - for the same underlying SST

anomalies. An interpretation consistent with this behaviour is that the SST-restoring acts as a constant source of heat in the Tropical North Atlantic in this region, such that the positive surface heat-fluxes (out of the ocean; c.f. Figs. 1j, k, m, n & 2h) support more intense convection (and associated heating) in the atmosphere of the Tropical North Atlantic. In the absence of active SST-restoring, positive SST anomalies on average support increased precipitation in the Tropical North Atlantic, however, in the absence of restoring heat-flux there are no upward surface heat fluxes to support any strong precipitation response. Similar results are found for an index of the inter-hemispheric SST gradient (shown in Supplementary Fig. 13) with a higher sensitivity of precipitation to the inter-hemispheric SST gradient found in the experiments with active SST-restoring (i.e. AMV and AMV-Trop). Therefore, the SST-restoring in the Tropical North Atlantic seems crucial for driving the strong positive surface heat-fluxes associated with warm SSTs, which is inconsistent with those seen in free-running models and observational data, and that these positive surface heat-fluxes are responsible for the stronger precipitation response seen in the SST-restoring experiments.

Remote decadal links between the North Atlantic and Pacific

To assess the remote influence of the AMV in the different experiments we now analyse the large-scale atmospheric circulation anomalies in these experiments. We first focus on the influence of the AMV on the Pacific Walker circulation, which has been highlighted in several previous studies. The decadal Pacific walker circulation anomalies (defined as the SLP difference across the Indo-Pacific region, following e.g. Vecchi et al.⁴²) are shown in Fig. 4. For the experiments with active SST-restoring in the Tropical North Atlantic, AMV & AMV-Trop, there is a significant strengthening of the Pacific Walker circulation on average, in response to the positive SST anomalies. The anomalous La Nina-like SST anomalies seen in the Tropical Pacific in these simulations (i.e. Fig. 1a, b, d, e) and in similar SST-restoring simulations are consistent with coupling to the strengthened Pacific Walker circulation and associated Trade winds^{33,35}. In contrast, there are much weaker anomalies in the AMV-ExTrop experiments with no significant changes in either of the experiments. The free-running simulations systematically show the opposite link to the AMV, with positive SST anomalies associated with a weakening of the Pacific Walker circulation and El Nino-like SST anomalies in the Tropical Pacific (i.e. Figs. 1c, f, i & S14, S15); there is no clear seasonal dependence on the sign of the response, though the changes are generally stronger during the boreal winter (Supplementary Fig. 16). This varies somewhat depending on the defined AMV region, however, overall it is evident that the strengthening of the Pacific Walker circulation in the AMV and AMV-Trop experiments is clearly not favoured in the free-running simulations, despite the presence of similar SST anomalies.

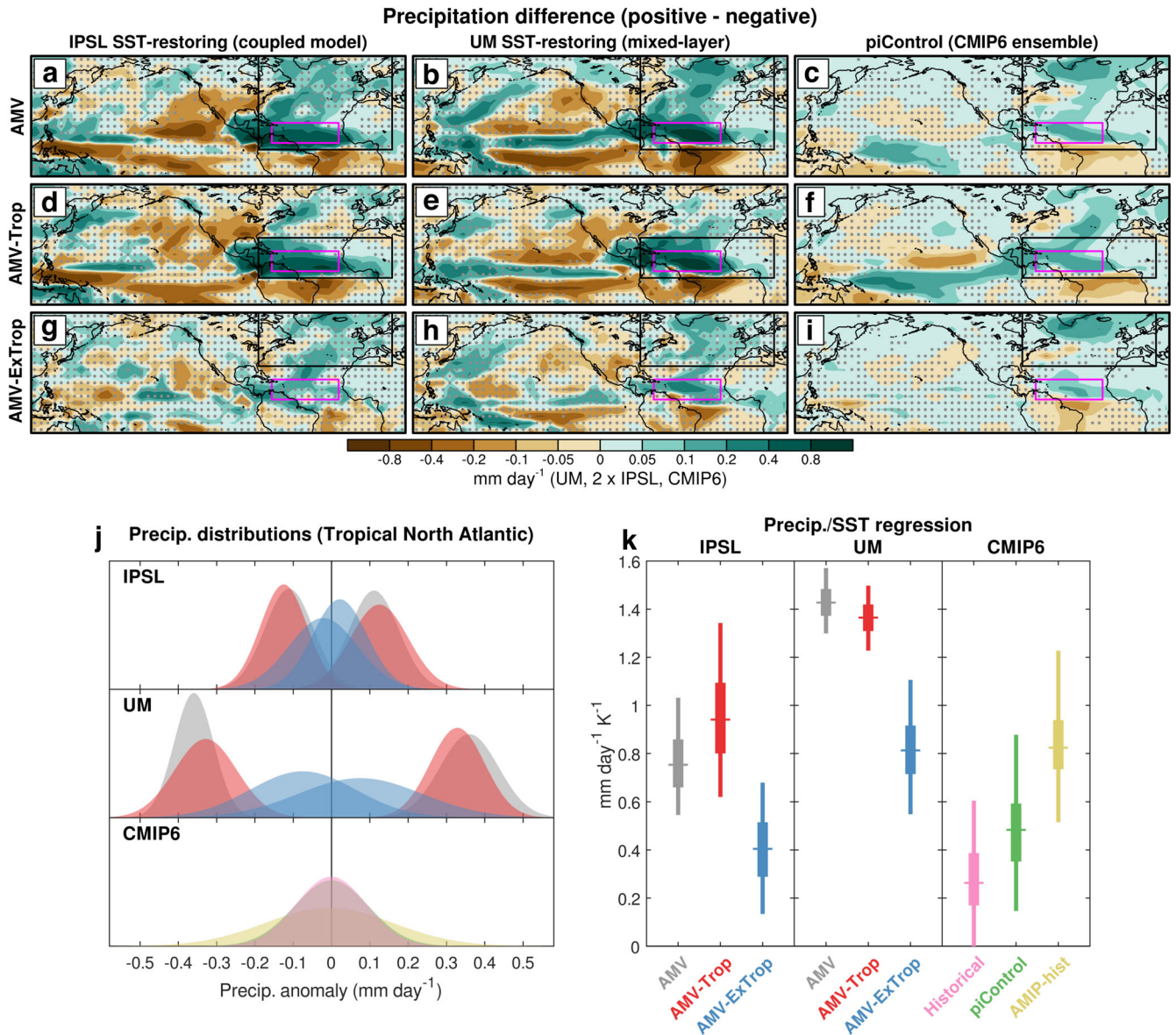


Fig. 3 Relationships between precipitation and the AMV. **a–i** Precipitation difference between SST+ and SST- 10-year periods for the AMV, AMV-Trop and AMV-ExTrop regions (indicated by the black boxes). These are shown for the SST-restoring experiments for the IPSL and UM models; for the free-running coupled PiControl simulations the SST+ and SST- decades are decades in which the SST in the region is above/below one standard deviation from the mean. Hatching indicates where the differences are significant at the 95% level, based on a Monte Carlo resampling performed 10000 times (see Methods). **j** Gaussian distributions of the decadal tropical North Atlantic precipitation anomalies in the different ensembles (averaged over the regions shown by the magenta boxes in panels (a–i)). **k** Regression of decadal precipitation anomalies onto decadal SST anomalies for the subtropical North Atlantic region. The regressions were calculated for all unique 140-year periods in the historical and piControl simulations and the box, centre-line and whiskers show the 5th-25th-50th-75th-95th percentiles of these distributions. For the SST-restoring experiments 10,000 random 140-year periods (i.e. 14 decades) were sampled and constructed from the ensemble members to calculate the regression; the box and whiskers show the distribution across these random samples for each experiment.

In the free-running coupled models, there is substantial spread in the relationship between SST and heat-flux in the subtropical North Atlantic (i.e. Figs. 2f, S3g), indicating that decades with positive SST and surface heat-flux can occur despite not dominating the overall relationship (as in the AMV and AMV-Trop experiments). Therefore, it is of interest to examine the periods in the free-running simulations in which the SST and heat-flux are both positive or negative and compare these with the SST-restoring experiments. Composite differences between positive SST/heat-flux decades and negative SST/heat-flux decades in the subtropical North Atlantic (shown in Supplementary Fig. 17) reveal that, despite the positive heat-flux anomaly, there are El Niño-like

SST anomalies in the Tropical Pacific and an anomalously weak Pacific Walker circulation, very similar to the full AMV differences (i.e. Figs. 1c, f, i & S14, S15). Therefore, even when positive SSTs occur in conjunction with positive heat-fluxes in the free-running models they do not resemble the large-scale global patterns seen in the SST-restoring experiments and might instead be associated with variability local to the Tropical North Atlantic that does not influence the Tropical Pacific.

The strength of the response of the Tropical Pacific in the SST-restoring experiments has been linked to the injection of moist static energy into the upper troposphere through deep convection over the Tropical North Atlantic in the multi-model study by

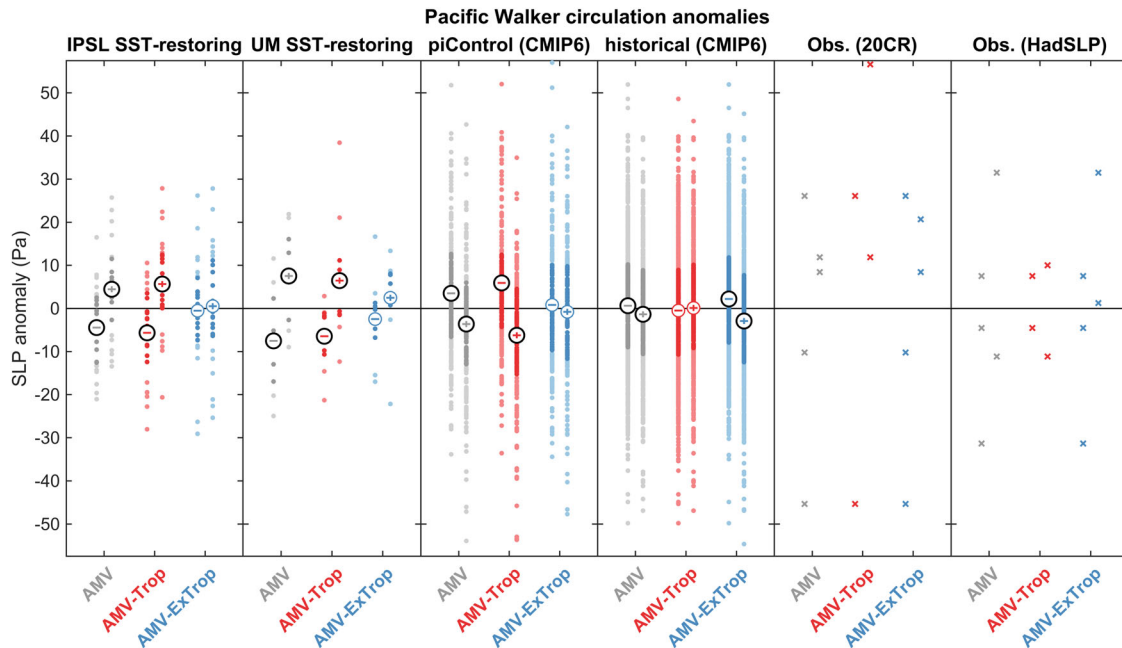


Fig. 4 Relationships between the Pacific Walker Circulation and the AMV. Decadal Pacific Walker circulation anomalies for SST+ and SST- ensembles for the SST-restoring simulations. Also shown are the equivalent for the SST+ and SST- periods from the free-running historical and piControl CMIP6 simulations. Each dot indicates a single decadal period from one simulation, the darker shading indicates the interquartile range of the distributions and the circles with the “plus” and “minus” signs show the ensemble mean anomalies for the SST+ and SST- ensemble simulations, respectively. The circles surrounding the “plus” and “minus” signs are black and emboldened when the difference in the ensemble mean are significantly different at the 95% level based on a t-test. The equivalent data points are also shown for two observational datasets, 20CR and HadSLP2, with each decade shown by a cross.

Ruprich-Robert et al.³⁵. The results presented here show the strongest precipitation anomalies over the Tropical North Atlantic in the AMV and AMV-Trop experiments are associated with a strengthening of the Pacific Walker circulation, whereas the weaker precipitation anomalies seen in the AMV-ExtTrop and the free-running coupled simulations are not associated with any strengthening of the Pacific Walker circulation. In the AMV and AMV-Trop experiments the active SST-restoring in the subtropics seems to be essential to drive the strong positive surface heat-fluxes (from positive SST anomalies) in the subtropical North Atlantic; these are in turn responsible for driving the strongest precipitation anomalies and the remote response in the Tropical Pacific. The systematically positive surface heat-flux anomalies driving the precipitation anomalies are inconsistent with the behaviour seen in free-running coupled model simulations and also with the observational estimates, which suggests that the influence of the AMV on the Tropical Pacific is unrealistic in the AMV and AMV-Trop SST-restoring experiments.

Examining the role of the Tropical Atlantic in recent multidecadal SST trends

The use of SST-relaxation experiments has been used in the Tropical Atlantic region to examine the role of the North Atlantic on global warming patterns. One notable study by Li et al.³⁴ used experiments with SST-restoring in several regions and compared the responses to SST trends over recent decades and found that the SST-restoring over the Tropical Atlantic compared well with the observed warming pattern. Our analysis to this point indicates that SST-restoring in the Tropical Atlantic and the associated surface heat-fluxes may lead to unrealistic results, so in light of this it is of interest to re-visit the role of the Tropical Atlantic in recent trends. To do so we analyse two transient pacemaker experiments with SST-restoring in the North Atlantic and Tropical Pacific, respectively, as well as the corresponding CMIP6 historical simulations (all from the IPSL-CM6-LR climate model).

The observed SST trend over the period 1979–2012 (following Li et al.³⁴), along with the ensemble mean SST trends from the Historical, North Atlantic and Tropical Pacific pacemaker simulations, are shown in Fig. 5a–d (equivalent maps of the surface heat-flux trends are shown in Supplementary Fig. 18). The distinct SST trend pattern in the observations, with warming across the entire North Atlantic and cooling across much of the Tropical Pacific, is not replicated in either the Historical ensemble or the North Atlantic pacemaker ensemble, which both have warming across the Tropical and North Pacific. However, the observed SST trend pattern in the Tropical Pacific pacemaker ensemble is very similar to the observed SST trend across the Tropical Pacific and the North Atlantic. The importance of the Tropical Pacific for the trends over this period was previously demonstrated by Kosaka and Xie³¹, who found this was particularly important for the reduced rate of global warming during the “hiatus” period. The dissimilarity of the SST trends in the North Atlantic pacemaker ensemble and observations initially appears to contradict the results of Li et al.³⁴. However, Li et al.³⁴ did not use a transient pacemaker setup but instead used an idealised SST-restoring experiment forced towards an SST anomaly pattern matching the observed trend, very similar to the SST-restoring experiments analysed above. By scaling the IPSL SST-restoring AMV experiment (i.e. Fig. 1a) to approximately match the magnitude of the observed trend over the North Atlantic - shown in Fig. 5e - we recover the results of Li et al.³⁴, with a global SST trend pattern that is similar to the observations.

So why are the AMV SST-restoring and North Atlantic pacemaker SST trends so different? To explore this we consider a simple toy-model of the SST anomaly in the subtropical North Atlantic (see Methods). The SST anomaly evolution and equivalent restoring heat-flux from integrating this toy-model are shown in Fig. 5f, g. Shown are results for two different experimental setups in the toy model: the first is a SST-restoring setup, which is the difference between two integrations - one targeting a positive anomaly and

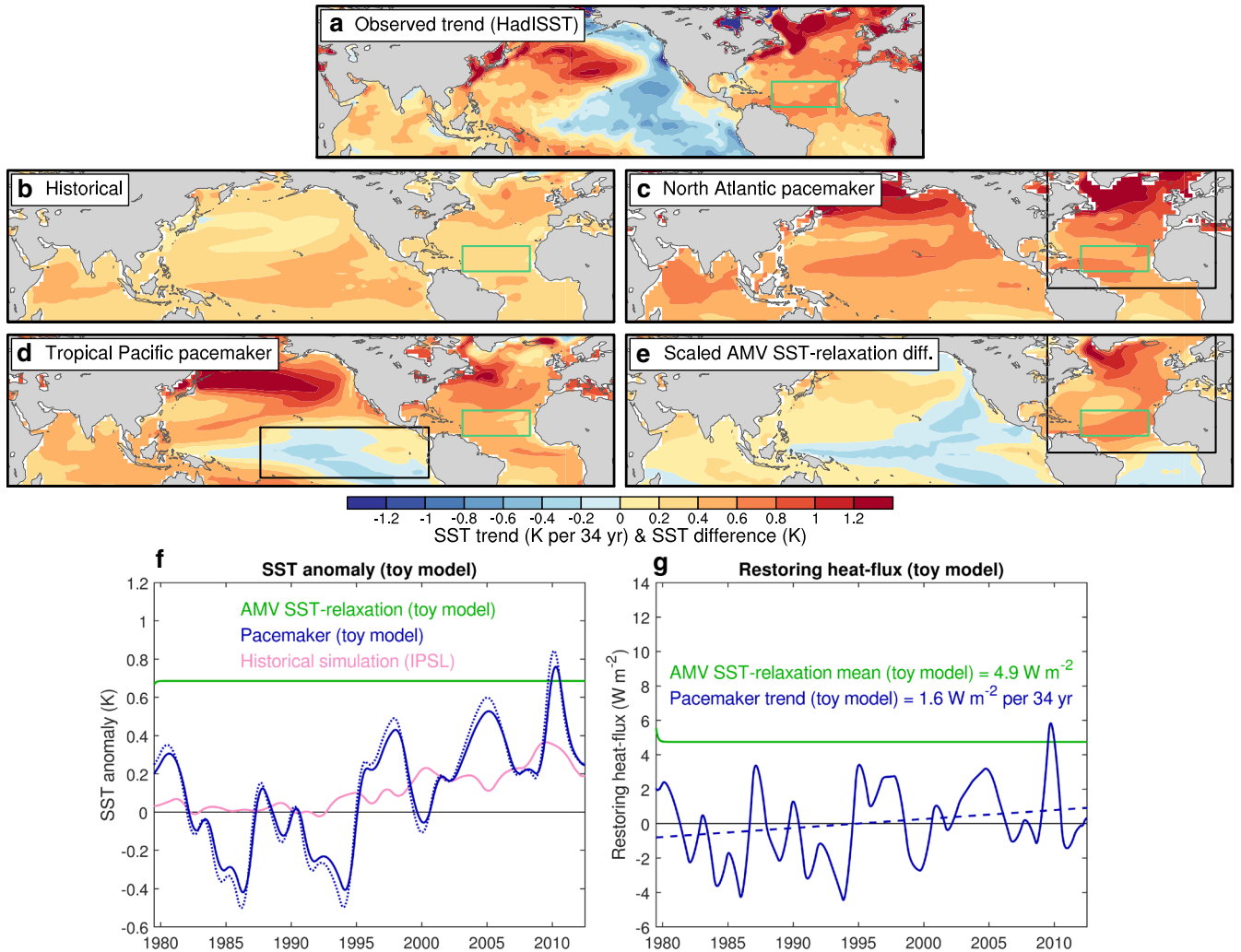


Fig. 5 Examining the role of the North Atlantic in controlling global SST trends over recent decades. SST trend over the period 1979–2012 in (a) observed SSTs from HadISST; (b) Historical IPSL ensemble mean; (c) North Atlantic IPSL pacemaker ensemble mean; (d) Tropical Pacific pacemaker ensemble mean; (e) Scaled IPSL SST-relaxation difference (i.e. scaled version of Fig. 1a). (f) Subtropical SST anomaly evolution from the SST-restoring toy model discussed in the text (examining the trend and effective trend shown in panels (c) & (e)), shown for an idealised AMV SST-relaxation simulation, North Atlantic pacemaker, along with the ensemble mean subtropical SST anomaly from the IPSL historical simulation. (g) Restoring heat-flux evolution for the toy model simulations shown in (f); the dashed line shows the toy model pacemaker trend.

one targeting a negative anomaly; the second is a transient pacemaker setup that targets an evolving prescribed SST anomaly, as in the transient pacemaker experiment shown in Fig. 5c. In these toy-model simulations the target SSTs are the observed SSTs in the case of the pacemaker and the constant equivalent trend in the case of the SST-restoring simulation (i.e. Fig. 5e).

In the transient pacemaker toy model, the restoring heat-flux trend (1.6 W m^{-2} per 34 yr) is around three times weaker than the constant restoring heat-flux (4.9 W m^{-2}) in the SST-restoring toy model. This is in part because the SST in the Historical simulation exhibits a similar positive trend to the observations so less restoring heat-flux is required to follow the target temperature. In the proper SST-restoring experiments, the restoring heat-flux in the subtropics (i.e. AMV and AMV-Trop experiments) clearly drives anomalous surface heat-flux to the atmosphere (e.g. Fig. 2). The scaled heat flux corresponding to the equivalent warming trend (i.e. Fig. 5e) is about 5 W m^{-2} , which is similar to the restoring heat-flux toy model (4.9 W m^{-2}). In the North Atlantic transient pacemaker experiment (i.e. Fig. 5c), the subtropical surface heat-flux trend is $-1.2 \pm 2.9 \text{ W m}^{-2}$ per 34 year, which is not substantially different from zero and is consistent with the weak

trend estimated from the toy model. The observational heat-flux estimate shows negative surface heat-flux trends over the subtropical North Atlantic region in recent decades (Supplementary Fig. 18); whilst this is quite noisy and uncertain, it is consistent with other observational analysis⁴³. In the transient pacemaker, the restoring heat-flux is seemingly very weak compared to internal variability (and possibly externally forced surface heat-flux variability) and therefore the positive surface heat-flux that is present in the constant SST-restoring experiment - which is crucial for generating the remote response in the Tropical Pacific - is not present in the North Atlantic pacemaker experiment and there is a much weaker remote influence on the Pacific. The difference between the subtropical North Atlantic surface heat-flux in the transient pacemaker and the constant SST-restoring experiments can therefore explain the discrepancy in the pattern of the SST trends between these two approaches.

DISCUSSION

In this study we have analysed the role of ocean-atmosphere interaction in the AMV and how this is represented in SST-

restoring simulations, free-running coupled model simulations and observations. Whilst both SST-restoring simulations and free-running models exhibit broadly similar North Atlantic SST anomalies, the experiments with active SST-restoring in the Tropical North Atlantic exhibit strong positive surface heat-fluxes with warm SST anomalies. However, the other simulations, the AMV-ExTrop experiments and the free-running coupled models, as well as the limited observational data, demonstrate weakly negative surface heat-fluxes associated with warm SST anomalies in the subtropical North Atlantic. Moreover, the positive surface heat-fluxes driven by the active SST-restoring in the Tropical North Atlantic are found to be crucial for generating a strong precipitation response in the Tropical North Atlantic and the associated remote impact on the large-scale Pacific Walker circulation, which are both absent in the simulations without active SST-restoring and that more closely resemble the limited observational data. Our results suggest that previous studies that invoke the Tropical Atlantic as an important driver of the recent multidecadal SST trends in the Tropical Pacific likely exaggerate the influence of the Atlantic due to the incorrect sign of the surface heat fluxes in the experiments with active SST-restoring in the Tropical Atlantic.

To consider why the SST-restoring in the tropics leads to seemingly unrealistic results it is useful to revisit mechanisms that have been linked to North Atlantic SST anomalies in the literature. Studies using models and observations have shown that anomalous ocean heat flux convergence in the midlatitudes contributes to changes in the ocean heat content and associated SST anomalies^{3,11,44}, linked to changes in the circulation of the horizontal gyres^{45,46} and the Atlantic Meridional Overturning Circulation^{47,48}. However, the SSTs in the subtropical branch of the AMV are typically more intermittent and are largely consistent with being forced by surface heat-fluxes^{49,50}, with the basin-wide coherency resulting from a remote teleconnection from the midlatitudes and are amplified by local feedbacks that do not directly depend on ocean circulation^{51–54}. In fully-coupled models and in available observational data, there are surface heat-flux out of the ocean in the midlatitudes^{55–57}, consistent with ocean heat convergence in this region, whereas in the tropics the heat fluxes are weakly negative and into the ocean (e.g. Fig. 1), consistent with being driven by atmospheric processes. The systematically strong upward subtropical surface heat-flux associated with the positive AMV in the AMV and AMV-Trop experiments is therefore seeming inconsistent with the mechanisms responsible for generating the AMV. As highlighted in the above analysis, periods in which there are upward surface heat-flux in the subtropical North Atlantic associated with positive SSTs do occur in the coupled models but these are associated with a weakening of the Pacific Walker circulation - the opposite of that seen in the SST-restoring experiments - and more likely reflect warm subtropical North Atlantic SST anomalies, driven by the Tropical Pacific changes, being damped to the atmosphere.

The results of this study strongly suggest that experiments employing SST-restoring (or prescribed SST boundary conditions) in the Tropical North Atlantic are likely to exaggerate the influence of SSTs in this region on global climate. In particular the remote impacts of the AMV in these experiments, such as those examined here and elsewhere showing the impact on Indo-Pacific SSTs³⁴, rely strongly on the SST-restoring in the Tropical North Atlantic - this is an important result and means that the results from these experiments should be treated with a degree of caution. The strong influence on the Tropical Pacific is particularly problematic because changes in the SSTs here can themselves generate strong remote teleconnections. For example, a remarkable result in the multi-model study of Ruggieri et al.⁵⁸ was that the most consistent feature of the extratropical circulation response to the AMV in SST-restoring experiments was the strong weakening of the Aleutian Low in the North Pacific, with less consistent response in the

extratropical North Atlantic. However, the strong weakening of the Aleutian Low is only found when SST-restoring is applied in the Tropical North Atlantic (i.e. AMV and AMV-Trop, see Supplementary Fig. 14), which our study indicates has an unrealistic influence on the local and remote atmospheric response.

It is important to highlight that the use of SST-restoring or prescribed SSTs in the Tropical Atlantic to understand the influence of the North Atlantic has been used widely, with at least 90 published studies based on experiments using such approaches (see Supplementary Text for a non-exhaustive list). However, our findings certainly do not suggest that SST-restoring is not a useful approach and there are many instances where it is likely to be insightful. For example, here we show that applying SST-restoring in the midlatitude North Atlantic (as in the AMV-ExTrop experiments) or by applying the restoring seasonally where appropriate (i.e. in the Tropical North Atlantic in boreal summer; Supplementary Figs. 11 & 12) would be well justified. SST-restoring experiments in the tropical North Atlantic are likely to be more useful on interannual timescales, when the Tropical Atlantic can have a clearer influence⁵⁹. The issues highlighted over the Tropical Atlantic in this study may have implications for experiments in which SST-restoring is applied over the Indian Ocean, which might similarly exaggerate the remote influence of the SST anomalies⁶⁰. Our findings suggest that experimental setups that are more cautious with where the SST-restoring is applied would avoid exaggerating the influence of the Tropical Atlantic and be more suitable for understanding the role of AMV in the global climate system.

METHODS

SST-restoring experiments

In this study we examine output from two models that both performed a full set of SST-restoring experiments, following the DCP-C experiments outlined in Boer et al.³². The first is the IPSL-CM6 fully-coupled ocean-atmosphere model ("IPSL SST-restoring" hereafter) and the second is the MetUM-GOML, which is the Global Ocean Mixed-Layer coupled configuration of the Met Office Unified Model ("UM SST-restoring" hereafter; Hirons et al.⁶¹). In these SST-restoring experiments, the model SST (i.e. within the ocean model component) is nudged towards either a positive or negative observed AMV anomaly pattern, over the following regions:

- *AMV*: The entire North Atlantic region (0–65°N; 80–0°W).
- *AMV-Trop*: The subtropical North Atlantic region (0–30°N; 80–0°W).
- *AMV-ExTrop*: The extratropical North Atlantic region (30–60°N; 80–0°W).

The target SST anomalies are constant and are added to a climatologically varying SST pattern. Further details on the application of the SST-restoring method are provided in the "Technical Note For DCP-Component C" (<https://www.wcrp-climate.org/wgsp/documents/Tech-Note-2.pdf>). For the IPSL pacemaker experiments there are 25 ensemble members for both positive/negative SST anomalies. For the UM pacemaker experiments there are 10 ensemble members for both positive/negative SST anomalies. All simulations last for 10-years. In the UM pacemaker experiments the magnitude of the SST pattern is doubled to increase the signal to noise ratio²⁶ - for this reason the IPSL results are shown with a different scaling (i.e. ×2) on some of the plots.

Free-running climate model simulations

We also use data from models simulations from the Coupled Model Intercomparison Project 6 (CMIP6) archive⁶². We analyse data from 318 different CMIP6 *Historical* simulations (between

1870–2014, to match the HadISST observational dataset) from 33 different models, totalling $\approx 46,000$ years of model data. We also analyse data from CMIP6 *piControl* simulations from 16 different models, all of which have at least 250 years of data and several have over 1000 years of data, totalling $\approx 11,500$ years of model data. For both Historical and *piControl* simulations we chose to use all models that were available which had complete data for all the variables required for the analysis in this study.

From the *piControl* simulations we define simple analogues to compare with the SST-restoring simulations by calculating SST indices over the regions corresponding to the AMV, AMV-Trop and AMV-ExTrop relaxation in the SST-restoring simulations (as defined above). For these analogues we define a positive/negative decade as one in which the SST anomaly averaged over that region exceeds a magnitude of 1 standard deviation (defined for each simulation separately, shown for the AMV region in Supplementary Fig. 1). Whilst other papers have considered different definitions of the AMV (or AMO in some studies), such as removing a global mean signal⁶³, here we take the simplest approach to most cleanly compare to the SST-restoring simulations. As a result, there appears to be a global mean SST signal that appears in the *piControl* composites, possibly due to the aliasing (or contribution) of the AMV to the global mean surface temperature that has been previously documented in the CMIP6 *piControl* simulations⁶⁴.

To complement the coupled model simulation we also use data from the AMIP-hist simulations from the CMIP6 archive, which allow us to understand how the atmosphere responds to SSTs in the absence of any oceanic response to the atmosphere. These simulations are an extended version of the Atmospheric Model Intercomparison Project (AMIP) simulations forced with prescribed observed SST boundary conditions over the period 1870–2014. We analyse data from 49 different AMIP-hist simulations.

Transient pacemaker experiments

For the final part of the Results section we examine trends from two transient pacemaker experiments using the IPSL-CM6 model. These simulations are the same as for the Historical CMIP6 simulations but with SSTs in (i) the North Atlantic and (ii) the Tropical Pacific, forced towards an 12-month low-pass filtered temperature anomaly taken from observations following the DCPD experimental protocol³². These transient pacemaker experiments are different from the SST-restoring experiments in that the SST target pattern is constantly evolving, whereas the target SSTs are fixed in the SST-restoring experiments. The transient pacemaker experiments also have evolving external forcing (as in the Historical CMIP6 simulations), whereas the SST-restoring experiments have fixed external forcing. Each of the transient pacemakers was performed with 10 ensemble members over the period 1920–2014.

Observational datasets

In addition to the model simulations we analyse observational SST data from the HadISST dataset⁶⁵, which is available from 1870. We use sea-level pressure (SLP) data from the HadSLP2 dataset⁶⁶, which is a gridded dataset produced using a statistical optimal interpolation method. We also use SLP and surface heat-flux data from the 20th Century Reanalysis (20CR) v3 dataset^{67,68}, which is a reanalysis dataset which only assimilates surface pressure observations and is forced by observed SSTs at the lower boundary.

The heat-flux from the 20CR dataset should be treated with some caution because it is a derived indirectly from the assimilating model rather than from direct observations (as in other reanalysis products) and because the number of observations in the subtropical North Atlantic is substantially less than in the midlatitudes. However, the constraint of the large-scale

atmospheric circulation at the surface and the SST boundary condition from below can provide useful constraints, as demonstrated by comparison to direct observational estimates by⁵⁵. The impact of the assimilated observations can be estimated by comparing the 20CR results to those of from the AMIP-hist simulations (i.e. in Fig. 2), which are in some ways similar to a reanalysis like but with the absence of any observational assimilation and merely forced by prescribed SSTs from observations. In the Tropical North Atlantic the 20CR and AMIP-hist simulations behave quite differently, indicating that the assimilation of the in-situ surface pressure observations plays an important role in determining the behaviour seen in 20CR.

The heat-flux data from 20CR has been compared with observations from the OAflux product⁶⁹ over the period 1958–2014. Overall, results similar to those from 20CR are found, particularly with regards to the relationship between heat-flux and SST in the midlatitude subtropical Atlantic regions, as shown in Supplementary Fig. 6.

In the analysis here we focus on 10-year (or decadal) means, following the length of the SST-restoring simulations. The datasets from the CMIP6 models and observations were converted into non-overlapping 10-year means. All the model and observational dataset were interpolated to a common regular $5^\circ \times 5^\circ$ resolution grid. The historical and observational datasets were linearly detrended prior to the analysis to be consistent with previous studies⁵⁵, however, the qualitative conclusions drawn here are not sensitive to this detrending.

Toy model of SST evolution

To analyse the influence of the SST-restoring heat-fluxes we use a simple toy-model of the SST anomaly, T' :

$$C \frac{\partial T'}{\partial t} = -\frac{C}{\tau_r} (T' - T'_{\text{target}}) - \frac{C}{\tau_{\text{clim}}} (T' - T'_{\text{clim}}), \quad (1)$$

where the first term on the r.h.s. is restoring heat-flux towards the target temperature anomaly on timescale $\tau_r = 60$ days (as in the SST-restoring experiments), the second term is a slower damping towards a background/climatological temperature on timescale $\tau_{\text{clim}} = 365$ days and C is the heat capacity of a mixed layer of depth 50m.

The model integrations in the text were performed by initialising the model at $T' = 0$ at the start of the integration in 1978. The model was then integrated forward until 2012 with a time-step of one day. For the SST-relaxation toy model runs, the T'_{target} was set to constant values of ± 0.4 with a background value of $T'_{\text{clim}} = 0$. The difference of these two runs was then calculated and is shown in Fig. 5g. For the transient pacemaker toy-model runs, the T'_{target} was set to the 12-month low-pass filtered observed SST (from HadISST) in the subtropical North Atlantic region. The background value, T'_{clim} was set to the 12-month low-pass filtered (25-member) ensemble mean SST from the CMIP6 Historical simulations from the IPSL model. The SST-restoring heat-flux was taken as the right hand side of equation (1). The conclusions are not overly sensitive to the relaxation timescales, with similar qualitative results found for $\tau_r < \tau_{\text{clim}}$, which is clearly justified based on the clear impact of the SST-relaxation in the SST-restoring and transient pacemaker experiments.

Significance testing and uncertainty estimates

We estimate significance of the differences between positive and negative AMV composites (i.e. Fig. 1) using a Monte Carlo resampling in which the positive and negative subsets are combined and then split into random subsets with the same numbers as the original subsets. The difference of these random subsets is recorded and the process repeated 10000 times to give a measure of the significance of the difference.

For the observational regression plots in Fig. 2 we use a Monte Carlo phase randomisation technique⁷⁰ which generates surrogate indices with the same spectral characteristics (and therefore similar autocorrelation) as the AMV index being analysed. The regression calculation is then repeated for 10,000 random indices to give an estimate of the significance level.

DATA AVAILABILITY

The model datasets used in this simulation are mostly available online from the CMIP6 archive. The only exception is data used from the UM simulations, which is available from COR on request. The observational datasets for SST, SLP and surface heat-fluxes are also all freely available online.

Received: 30 May 2022; Accepted: 8 February 2023;

Published online: 22 February 2023

REFERENCES

- Delworth, T. L. & Mann, M. E. Observed and simulated multidecadal variability in the Northern Hemisphere. *Clim. Dyn.* **16**, 661–676 (2000).
- Enfield, D. B., Mestas-Nuñez, A. M. & Trimble, P. J. The Atlantic Multidecadal Oscillation and its relation to rainfall and river flows in the continental US. *Geophys. Res. Lett.* **28**, 2077–2080 (2001).
- Knight, J. R., Allan, R. J., Folland, C. K., Vellinga, M. & Mann, M. E. A signature of persistent natural thermohaline circulation cycles in observed climate. *Geophys. Res. Lett.* **32**, 1–4 (2005).
- Ting, M., Kushnir, Y., Seager, R. & Li, C. Forced and internal twentieth-century SST trends in the North Atlantic. *J. Clim.* **22**, 1469–1481 (2009).
- McCabe, G. J., Palecki, M. A. & Betancourt, J. L. Pacific and Atlantic ocean influences on multidecadal drought frequency in the United States. *Proc. Natl Acad. Sci.* **101**, 4136–4141 (2004).
- Sutton, R. T. & Hodson, D. L. Atlantic ocean forcing of North American and European summer climate. *Science* **309**, 115–118 (2005).
- Hodson, D. L. et al. Climate impacts of recent multidecadal changes in Atlantic Ocean sea surface temperature: A multimodel comparison. *Clim. Dyn.* **34**, 1041–1058 (2010).
- Ting, M., Kushnir, Y., Seager, R. & Li, C. Robust features of Atlantic Multi-decadal Variability and its climate impacts. *Geophys. Res. Lett.* **38**, L17705 (2011).
- Nigam, S., Guan, B. & Ruiz-Barradas, A. Key role of the Atlantic Multidecadal Oscillation in 20th century drought and wet periods over the Great Plains. *Geophys. Res. Lett.* **38**, L048650 (2011).
- Ruprich-Robert, Y. et al. Impacts of the Atlantic Multidecadal Variability on North American summer climate and heat waves. *J. Clim.* **31**, 3679–3700 (2018).
- Zhang, R. et al. A review of the role of the Atlantic Meridional Overturning Circulation in Atlantic Multidecadal Variability and associated climate impacts. *Rev. Geophys.* **57**, 316–375 (2019).
- Sutton, R. & Hodson, D. Influence of the ocean on North Atlantic climate variability 1871–1999. *J. Clim.* **16**, 3296–3313 (2003).
- Sutton, R. T. & Dong, B. Atlantic Ocean influence on a shift in European climate in the 1990s. *Nat. Geosci.* **5**, 788–792 (2012).
- O'Reilly, C. H., Woollings, T. & Zanna, L. The dynamical influence of the Atlantic Multidecadal Oscillation on continental climate. *J. Clim.* **30**, 7213–7230 (2017).
- Ghosh, R., Müller, W. A., Baehr, J. & Bader, J. Impact of observed North Atlantic multidecadal variations to European summer climate: A linear baroclinic response to surface heating. *Clim. Dyn.* **48**, 3547–3563 (2017).
- Qasmi, S., Cassou, C. & Boé, J. Teleconnection processes linking the intensity of the Atlantic Multidecadal Variability to the climate impacts over Europe in boreal winter. *J. Clim.* **33**, 2681–2700 (2020).
- Folland, C. K., Palmer, T. N. & Parker, D. E. Sahel rainfall and worldwide sea temperatures, 1901–85. *Nature* **320**, 602–607 (1986).
- Zhang, R. & Delworth, T. L. Impact of Atlantic Multidecadal Oscillations on India/Sahel rainfall and Atlantic hurricanes. *Geophys. Res. Lett.* **33**, L17712 (2006).
- Mohino, E., Janicot, S. & Bader, J. Sahel rainfall and decadal to multi-decadal sea surface temperature variability. *Clim. Dyn.* **37**, 419–440 (2011).
- Martin, E. R., Thorncroft, C. & Booth, B. B. The multidecadal Atlantic SST-Sahel rainfall teleconnection in CMIP5 simulations. *J. Clim.* **27**, 784–806 (2014).
- Lu, R., Dong, B. & Ding, H. Impact of the Atlantic Multidecadal Oscillation on the Asian summer monsoon. *Geophys. Res. Lett.* **33**, L02706 (2006).
- Zhang, R. & Delworth, T. L. Impact of the Atlantic Multidecadal Oscillation on North Pacific climate variability. *Geophys. Res. Lett.* **34**, L031601 (2007).
- Ruprich-Robert, Y. et al. Assessing the climate impacts of the observed Atlantic Multidecadal Variability using the GFDL CM2.1 and NCAR CESM1 global coupled models. *J. Clim.* **30**, 2785–2810 (2017).
- Sun, C. et al. Western Tropical Pacific multidecadal variability forced by the Atlantic Multidecadal Oscillation. *Nature communications* **8**, 1–10 (2017).
- Monerie, P.-A., Robson, J., Dong, B. & Dunstone, N. A role of the Atlantic Ocean in predicting summer surface air temperature over North East Asia? *Clim. Dyn.* **51**, 473–491 (2018).
- Monerie, P., Robson, J. & Dong, B. et al. Effect of the Atlantic Multidecadal Variability on the global monsoon. *Geophys. Res. Lett.* **46**, 1765–1775 (2019).
- Sutton, R. T. & Hodson, D. L. Climate response to basin-scale warming and cooling of the North Atlantic ocean. *J. Clim.* **20**, 891–907 (2007).
- Wang, Y., Li, S. & Luo, D. Seasonal response of Asian monsoonal climate to the Atlantic Multidecadal Oscillation. *J. Geophys. Res. Atmos.* **114**, D02112 (2009).
- Simpkins, G. R., McGregor, S., Taschetto, A. S., Ciasto, L. M. & England, M. H. Tropical connections to climatic change in the extratropical Southern Hemisphere: The role of Atlantic SST trends. *J. Clim.* **27**, 4923–4936 (2014).
- Barsugli, J. J. & Battisti, D. S. The basic effects of atmosphere–ocean thermal coupling on midlatitude variability. *J. Atmos. Sci.* **55**, 477–493 (1998).
- Kosaka, Y. & Xie, S.-P. Recent global-warming hiatus tied to equatorial Pacific surface cooling. *Nature* **501**, 403–407 (2013).
- Boer, G. J. et al. The Decadal Climate Prediction Project (DCPP) contribution to CMIP6. *Geosci. Model Dev.* **9**, 3751–3777 (2016).
- Meehl, G. A. et al. Atlantic and Pacific tropics connected by mutually interactive decadal-timescale processes. *Nat. Geosci.* **14**, 36–42 (2021).
- Li, X., Xie, S.-P., Gille, S. T. & Yoo, C. Atlantic-induced pan-tropical climate change over the past three decades. *Nat. Clim. Chan.* **6**, 275–279 (2016).
- Ruprich-Robert, Y. et al. Impacts of Atlantic Multidecadal Variability on the Tropical Pacific: a multi-model study. *npj Clim. Atmos. Sci.* **4**, 1–11 (2021).
- Trascasa-Castro, P., Ruprich-Robert, Y., Castruccio, F. & Maycock, A. C. Warm phase of AMV damps ENSO through weakened thermocline feedback. *Geophys. Res. Lett.* **48**, e2021GL096149 (2021).
- Yao, S.-L., Zhou, W., Jin, F.-F. & Zheng, F. North Atlantic as a trigger for Pacific-wide decadal climate change. *Geophys. Res. Lett.* **48**, e2021GL094719 (2021).
- Hodson, D. L. et al. Coupled climate response to Atlantic Multidecadal Variability in a multi-model multi-resolution ensemble. *Clim. Dyn.* **59**, 1–32 (2022).
- Wang, C., Wang, B., Wu, L. & Luo, J.-J. A see-saw variability in tropical cyclone genesis between the western North Pacific and the North Atlantic shaped by Atlantic Multidecadal Variability. *J. Clim.* **1–37** (2022).
- Alexander, M. & Scott, J. The influence of ENSO on air-sea interaction in the Atlantic. *Geophys. Res. Lett.* **29**, 46–1 (2002).
- Chikamoto, Y., Johnson, Z., Wang, S.-Y. S., McPhaden, M. & Mochizuki, T. El Niño–Southern Oscillation evolution modulated by Atlantic forcing. *J. Geophys. Res. Oceans* **125**, e2020JC016318 (2020).
- Vecchi, G. A. et al. Weakening of Tropical Pacific atmospheric circulation due to anthropogenic forcing. *Nature* **441**, 73–76 (2006).
- Cook, K. H. & Vizy, E. K. Examining multidecadal trends in the surface heat balance over the tropical and subtropical oceans in atmospheric reanalyses. *Int. J. Climatol.* **40**, 2253–2269 (2020).
- Robson, J., Sutton, R., Lohmann, K., Smith, D. & Palmer, M. D. Causes of the rapid warming of the North Atlantic ocean in the mid-1990s. *J. Clim.* **25**, 4116–4134 (2012).
- Williams, R. G., Roussenov, V., Smith, D. & Lozier, M. S. Decadal evolution of ocean thermal anomalies in the North Atlantic: The effects of Ekman, overturning, and horizontal transport. *J. Clim.* **27**, 698–719 (2014).
- Buckley, M. W., Ponte, R. M., Forget, G. & Heimbach, P. Determining the origins of advective heat transport convergence variability in the North Atlantic. *J. Clim.* **28**, 3943–3956 (2015).
- Zhang, R. Coherent surface-subsurface fingerprint of the Atlantic Meridional Overturning Circulation. *Geophys. Res. Lett.* **35**, L035463 (2008).
- Moat, B. I. et al. Insights into decadal North Atlantic sea surface temperature and ocean heat content variability from an eddy-permitting coupled climate model. *J. Clim.* **32**, 6137–6161 (2019).
- Li, L., Lozier, M. S. & Buckley, M. W. An investigation of the ocean's role in Atlantic Multidecadal Variability. *J. Clim.* **33**, 3019–3035 (2020).
- Lai, W., Robson, J., Wilcox, L. & Dunstone, N. Mechanisms of internal Atlantic Multidecadal Variability in HadGEM3-GC3.1 at two different resolutions. *J. Clim.* **35**, 1365–1383 (2022).
- Xie, S.-P. A dynamic ocean–atmosphere model of the Tropical Atlantic decadal variability. *J. Clim.* **12**, 64–70 (1999).
- Clement, A. et al. The Atlantic Multidecadal Oscillation without a role for ocean circulation. *Science* **350**, 320–324 (2015).
- Yuan, T. et al. Positive low cloud and dust feedbacks amplify Tropical North Atlantic Multidecadal Oscillation. *Geophys. Res. Lett.* **43**, 1349–1356 (2016).

54. Oelsmann, J., Borchert, L., Hand, R., Baehr, J. & Jungclaus, J. H. Linking ocean forcing and atmospheric interactions to Atlantic Multidecadal Variability in MPI-ESM1.2. *Geophys. Res. Lett.* **47**, e2020GL087259 (2020).
55. Gulev, S. K., Latif, M., Keenlyside, N., Park, W. & Koltermann, K. P. North Atlantic ocean control on surface heat flux on multidecadal timescales. *Nature* **499**, 464–467 (2013).
56. O'Reilly, C. H., Huber, M., Woollings, T. & Zanna, L. The signature of low-frequency oceanic forcing in the Atlantic Multidecadal Oscillation. *Geophys. Res. Lett.* **43**, 2810–2818 (2016).
57. O'Reilly, C. H. & Zanna, L. The signature of oceanic processes in decadal extratropical SST anomalies. *Geophys. Res. Lett.* **45**, 7719–7730 (2018).
58. Ruggieri, P. et al. Atlantic Multidecadal Variability and North Atlantic jet: a multimodel view from the Decadal Climate Prediction Project. *J. Clim.* **34**, 347–360 (2021).
59. Ham, Y.-G., Kug, J.-S. & Park, J.-Y. Two distinct roles of Atlantic SSTs in ENSO variability: North Tropical Atlantic SST and Atlantic Niño. *Geophys. Res. Lett.* **40**, 4012–4017 (2013).
60. Copesey, D., Sutton, R. & Knight, J. R. Recent trends in sea level pressure in the Indian Ocean region. *Geophys. Res. Lett.* **33**, L19712 (2006).
61. Hiron, L., Klingaman, N. & Woolnough, S. MetUM-GOML1: a near-globally coupled atmosphere–ocean–mixed-layer model. *Geosci. Model Dev.* **8**, 363–379 (2015).
62. Eyring, V. et al. Overview of the Coupled Model Intercomparison Project phase 6 (CMIP6) experimental design and organization. *Geosci. Model Dev.* **9**, 1937–1958 (2016).
63. Deser, C. & Phillips, A. S. Defining the internal component of Atlantic Multidecadal Variability in a changing climate. *Geophys. Res. Lett.* **48**, e2021GL095023 (2021).
64. Parsons, L. A., Brennan, M. K., Wills, R. C. & Proistosescu, C. Magnitudes and spatial patterns of interdecadal temperature variability in CMIP6. *Geophys. Res. Lett.* **47**, e2019GL086588 (2020).
65. Rayner, N. et al. Global analyses of sea surface temperature, sea ice, and night marine air temperature since the late nineteenth century. *J. Geophys. Res. Atmos.* **108**, 4407–4443 (2003).
66. Allan, R. & Ansell, T. A new globally complete monthly historical gridded mean sea level pressure dataset (HadSLP2): 1850–2004. *J. Clim.* **19**, 5816–5842 (2006).
67. Compo, G. P. et al. The Twentieth Century Reanalysis Project. *Q. J. R. Meteorol. Soc.* **137**, 1–28 (2011).
68. Slivinski, L. C. et al. Towards a more reliable historical reanalysis: Improvements for version 3 of the Twentieth Century Reanalysis system. *Q. J. R. Meteorol. Soc.* **145**, 2876–2908 (2019).
69. Yu, L. & Weller, R. A. Objectively analyzed air–sea heat fluxes for the global ice-free oceans (1981–2005). *Bull. Am. Meteorol. Soc.* **88**, 527–540 (2007).
70. Ebisuzaki, W. A method to estimate the statistical significance of a correlation when the data are serially correlated. *J. Clim.* **10**, 2147–2153 (1997).

ACKNOWLEDGEMENTS

COR was supported by a Royal Society University Research Fellowship. MP was funded by the EUCP project (Horizon 2020; Grant Agreement 776613). JR was funded

by NERC via the ACSIS program (NE/N018001/1) and via the WISHBONE project (NE/T013516/1). PAM was funded by the EMERGENCE project under the Natural Environment Research Council (NERC Grant NE/S004890/1) The project that gave rise to these results included YRR and received the support of a fellowship from “la Caixa” Foundation (ID 100010434) and from the European Union’s Horizon 2020 research and innovation programme under the Marie Skłodowska-Curie grant agreement No 847648 (fellowship code LCF/BQ/PR21/11840016).

AUTHOR CONTRIBUTIONS

COR conceived of the study and performed the analysis. All authors contributed to the analysis of the results and the manuscript writing.

COMPETING INTERESTS

The authors declare no competing interests.

ADDITIONAL INFORMATION

Supplementary information The online version contains supplementary material available at <https://doi.org/10.1038/s41612-023-00335-0>.

Correspondence and requests for materials should be addressed to Christopher H. O'Reilly.

Reprints and permission information is available at <http://www.nature.com/reprints>

Publisher's note Springer Nature remains neutral with regard to jurisdictional claims in published maps and institutional affiliations.



Open Access This article is licensed under a Creative Commons Attribution 4.0 International License, which permits use, sharing, adaptation, distribution and reproduction in any medium or format, as long as you give appropriate credit to the original author(s) and the source, provide a link to the Creative Commons license, and indicate if changes were made. The images or other third party material in this article are included in the article's Creative Commons license, unless indicated otherwise in a credit line to the material. If material is not included in the article's Creative Commons license and your intended use is not permitted by statutory regulation or exceeds the permitted use, you will need to obtain permission directly from the copyright holder. To view a copy of this license, visit <http://creativecommons.org/licenses/by/4.0/>.

© The Author(s) 2023